EUROPEAN COMMISSION

Community Research

SEVENTH FRAMEWORK PROGRAMME

ARCHER

Collaborative Project (CP)

Co-funded by the European Commission under the Euratom Research and Training Programme on Nuclear Energy within the Seventh Framework Programme

Grant Agreement Number : 269892

Start date : 01/02/2011 Duration : 48 Months

www.archer-project.eu

Creep behaviour of coated particle layers through tomography

Authors : KNOL Steven (NRG) , S. Knol

ARCHER - Contract Number: 269892
Advanced High-Temperature Reactors for Cogeneration of Heat and Electricity R&D
EC Scientific Officer: Dr. Panagiotis Manolatos

Document title	Creep behaviour of coated particle layers through tomography
Author(s)	KNOL Steven , S. Knol
Number of pages	22
Document type	Deliverable
Work Package	WP 31
Document number	D31.11 rev. 1
Issued by	NRG
Date of completion	23/02/2015
Dissemination level	Confidential, only for members of the consortium (including the Commission Services).

Summary

This document contains the results from the X-Ray tomography investigations from the PYCASSO irradiation tests in the HFR Petten that have been completed as part of the RAPHAEL FP6 project, and disassembled with the coated particles being recovered. Creep and swelling properties of the coated layers due to the neutron dose will be the main focus of the PIE. NRG has purchased a high resolution X-Ray tomography equipment which can be used for detailed non-destructive analysis of the particles and coatings. This is an important breakthrough, as the device will be automated to permit the determination of the layer dimensions of a large number of coated particles. This report presents the results of the coating layer behavior.

Approval

Date	By
24/02/2015	Steven KNOL
16/03/2015	Mathias LAURIE
16/03/2015	Steven KNOL

Distribution list

Name	Organisation	Comments
P. Manolatos	EC DG RTD	Through the EC participant portal
All beneficiaries	ARCHER	Through the private online workspace

Table of contents

1 Summary 3
2 Introduction 4
3 PYCASSO Irradiations 5
3.1 Irradiation history 5
3.2 Sample specification 6
4 Measurements 8
4.1 Equipment 8
4.2 Particle handling 9
4.3 Measurement 10
4.4 Reconstruction and data analysis 10
4.4.1 Data preparation and segmentation 11
4.4.2 Data analysis 13
5 Results 14
5.1 PYC 1 14
5.2 PYC 2 16
6 Conclusions 20
7 Acknowledgement 20

1 Summary

This report describes the X-Ray tomography work that is done at NRG on the irradiated particles. It focuses on the knowledge on the densification kinetics by determining the swelling and shrinkage of the separate layers as a function of fluence. The particles investigated in this work are provided by CEA (France) and consist of various coating materials and combinations for TRISO coated particle fuel. Effects due to the presence of fuel, such as pressurization or chemical attack by fission products, have been excluded by irradiating surrogate (Al2O3) kernels. The PYCASSO irradiations were performed in the High Flux Reactor (HFR) Petten and were coordinated by NRG (The Netherlands).

Close to 500 particles have been measured by X-Ray Tomography at NRG. The results show consistent results with the coating sizes measured during fabrication, showing a consistent result between the two methods. The technique allows a large number of particles to be studied non-destructively, for which a batch process was developed and used. With this new process, it was made possible to scan particles continuously during day and night.

The XRT measurements were performed at NRG and data was analysed by the University of Manchester. The results show a clear difference between the two type of particles that were studies. The particles that consisted of a kernel, buffer layer and OPyC layer clearly showed shrinkage in the two graphite layers. The buffer is known to shrink, but without any restraint, the OPyC layer follows the buffer layer, shrinking up to 3.7% in radius, whilst increasing up to 3.5% in thickness.
For the second type of particle with a SiC layer between the two graphite layers, the SiC layer clearly restrains the OPyC layer. The buffer shows similar behaviour, shinking significantly in size, the SiC remains unchanged, also keeping the OPyC layer in place. In this case, the OPyC layer does shrink significantly in thickness, up to 6.75%.

2 Introduction

The PYCASSO (PYrocarbon irradiation for Creep And Swelling/Shrinkage of Objects) irradiations were a part of RAPHAEL (ReActor for Process Heat And ELectricity) [1], a 4-year Integrated Project on Very High Temperature Reactors, within the European 6th Framework Program. The work is continued within ARCHER [2] in which the Post Irradiation Examinations (PIE) are performed.

This report describes the X-Ray tomography work that is done at NRG on the irradiated particles. It focuses on the densification kinetics by determining the swelling and shrinkage of the separate layers as a function of fluence. The particles investigated in this work are provided by CEA (France) and consist of various coating materials and combinations for TRISO coated particle fuel. Effects due to the presence of fuel, such as pressurization or chemical attack by fission products, have been excluded by irradiating surrogate (Al2O3) kernels. The PYCASSO irradiations were performed in the High Flux Reactor (HFR) Petten and were coordinated by NRG (The Netherlands). In the next chapter the irradiation history will be explained further, including more detail on the particles. Chapter 4 will elaborate on the measurement technique, including the 3D image reconstruction and data analysis, which is performed by the X-Ray Imaging center of the University of Manchester. The results of the data analysis are presented in chapter 4.

3 PYCASSO Irradiations

The particles fabricated by CEA for the PYCASSO irradiations were designed to systematically investigate the densification kinetics of the pyrocarbon layers, in order to study the effects of relatively new fabrication processes. Dedicated particles have been manufactured consisting of surrogate kernels (Al_2O_3) with different types of PyC/SiC combinations, as shown in Figure 3-1. All specimens delivered have been extensively characterized during fabrication per production batch, providing a good reference for the post irradiation examinations. Results may be compared to behaviour of standard particles, such as the AVR-21-2 (LEU UO_2) TRISO particle which can be considered the current reference.

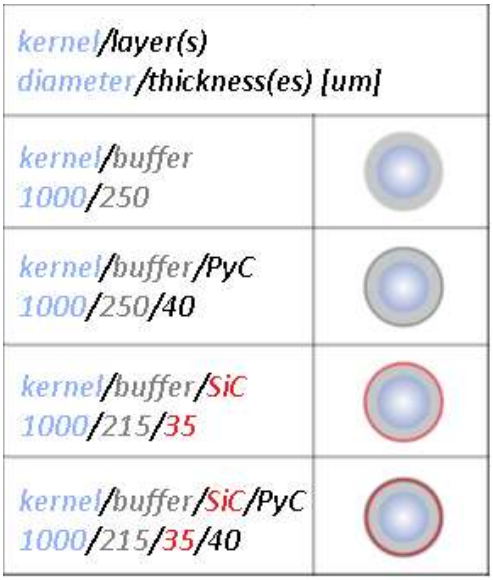

Figure 3-1: PYCASSO-I fabrication targets

3.1 Irradiation history

The CEA specimens were irradiated at a well-defined temperature (full temperature range 980-1020 °C) and excluded effects due to the presence of fuel, such as pressurization or chemical attack by fission products. These irradiations can therefore be considered separate effect tests, where only the influence of neutron fluence and temperature on coatings and coating combinations are investigated.
The samples were placed in heavy metal alloy discs to generate the heat, and allowed a large number of particles within one stack (see Figure 3-2). In PYCASSO-I the CEA particles were irradiated in two drums stacks, positioned at different elevations in the experiment. The irradiation took 5 HFR irradiation cycles, having a total of 144 full power irradiation days. This resulted in two different fluence levels of on average $2.05 \cdot 10^{25}$ m^{-2} and $1.65 \cdot 10^{25}$ m^{-2} ($E > 0.18$ MeV), these values are confirmed by post irradiation neutron metrology. For each separate tray and samples therein, the achieved fluence can be determined with high accuracy, which facilitates correlating material changes with fluence. The other stacks contained samples supplied by JAEA and KAERI. The samples consisted of a variety of materials and coating combinations for other research purposes. These stack were irradiated at different temperatures.
A detailed description of the PYCASSO samples and irradiation conditions can be found in references [3] and [4]. Figure 3-2 shows a top view of one of the discs, and an indication of the placement within the irradiation experiment.

Figure 3-2: PYCASSO I experiment after assembly of the inner parts

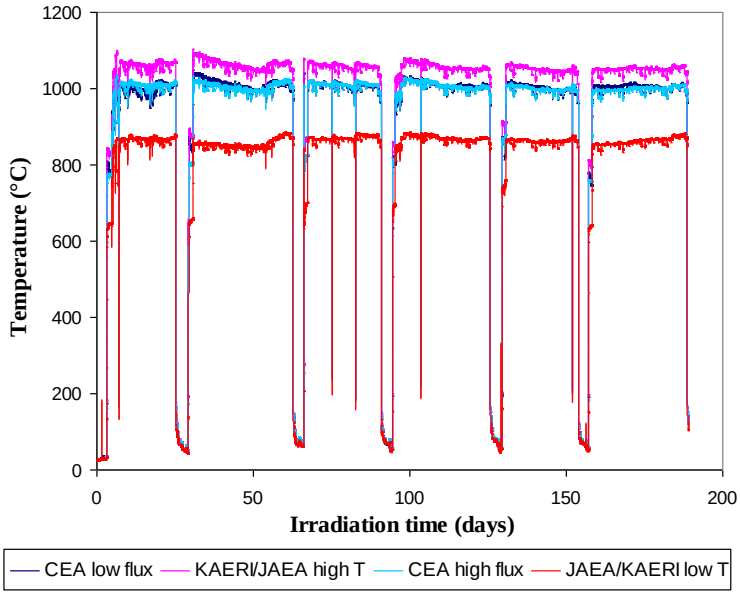

Figure 3-3: PYCASSO I Temperature readings

3.2 Sample specification

For the X-ray tomography measurements, two types of particles have been selected, irradiated to different fluence levels (see Table 3-1). The selected particles are the two types from Figure 3-1 with PyC on the outside. These are referred to as PyC1 (kernel/buffer/PyC) and PyC 2 (kernel/buffer/SiC/PyC).
The PyC1 particles were irradiated in the bottom CEA stack, disc number 6 (BC-6) and the middle CEA stack, disc number 6 (MC-6). The PyC2 particles were irradiated in discs numbers 12 and 2, of the bottom and middle stack, respectively. Additionally, unirradiated particles were measured, these are labelled with their fabrication code.

Table 3-1: Particles used for XRT measurements

Irradiation Code	Fabrication code	Coating layers	Particle Size [µm]	$\Phi_{E>0.18\,MeV}$ [$10^{24}m^{-2}$]	dpa in Carbon	Irradiation Temperatures [°C]
PYC1						
Unirradiated	PyC1-6_9	Kernel/buffer/PyC		-	-	-
PYC BC-6 "Low Fluence"	PyC 1 (3/9) B2	Kernel/buffer/PyC	1558	16.33	1.23	993.2
PYC MC-6 "High Fluence"	PyC 1 (1/9) B1	Kernel/buffer/PyC	1557	20.25	1.51	993.9
PYC2						
Unirradiated	PyC2-5_9	Kernel/buffer/SiC/PyC		-	-	-
PYC BC-12 "Low Fluence"	PyC 2 (3/9) B2	Kernel/buffer/SiC/PyC	1571	14.34	1.08	1016.0
PYC MC-2 "High Fluence"	PyC 2 (2/9) B1	Kernel/buffer/SiC/PyC	1573	19.97	1.49	989.2

All samples are characterized during the fabrication process at CEA. During fabrication the dimensions were optically measured between each coating step, determining the thickness of the added layer.

Table 3-2 shows the average layer dimensions measured after all fabrication step [3, 3]. Note that the dimensions are determined for each fabrication batch individually, the data reported here is averaged over all batches.

Table 3-2: Detailed sample characterization from fabrication report

Type of particle	Particle diameter (µm)	Layer thickness (µm)	Density of kernel/layer
Kernel	**992**	-	3.88
		Measured using metallography	
Kernel/buffer 1 Archiving sub-batch	**1460**	**223** σ = 11	1.1
Kernel/buffer/PyC1 Archiving sub-batch	**1553** σ = 22	**60** σ =3	1.95
Kernel/buffer 2 Archiving sub-batch	**1410** σ = 22	**187** σ =17	1.07
Kernel/buffer/SiC 2 Archiving sub-batch	**1489** σ = 21	**59** σ =3	3.16
Kernel/buffer/SiC/PyC 2 Archiving sub-batch	**1572** σ = 1	**39** σ =3	2.05

4 Measurements

4.1 Equipment

The X-ray tomography on graphite samples is performed on a GE Phoenix X-Ray Nanotom S tomograph system (see Figure 4-1). The Nanotom S has a 180 kV high-power nanofocus X-Ray tube (see Figure 4-2). The system works by focussing an electron beam on a target with a sub-micron spot size, creating a X-Ray cone beam. By placing a sample close to the source, the image is magnified on the detector screen. In combination with the high-contrast area detector, X-Ray images with a resolution down to 0.5 µm can be achieved. The achievable resolution depends on sample size and material. The Nanotom S is equipped with a "threefold virtual detector", i.e. a detector that can be moved back and forth to widen the field of view by up to a factor three. The virtual detector options allows for high resolution imaging on large samples. X-Ray images are acquired using the "datos|x acquisition" software on the control PC.

Figure 4-1 GE Phoenix X-Ray Nanotom S as used by NRG

The acquired X-Ray images are used to reconstruct a 3D volume of the object. The reconstructed volume represents a 3D mapping of the X-ray absorption coefficient of the inspected object. Reconstruction of X-Ray images into a 3D volume is performed by the software "datos|x reconstruction" on a dedicated workstation. The reconstruction workstation at NRG is equipped with dual graphical processing units (GPUs) and 128 GB RAM memory for fast reconstruction and large files.

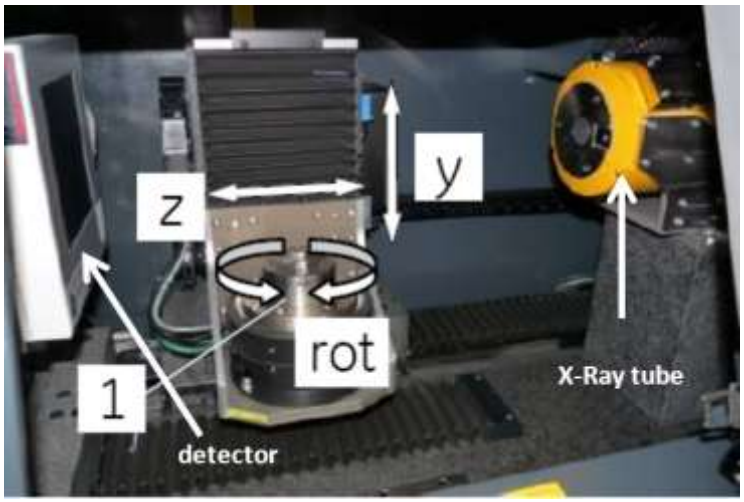

Figure 4-2: X-Ray Tube, sample manipulator, and area detector in the Nanotom S.

4.2 Particle handling

To process the large amount of particles, it was not feasible to place the samples one-by-one. Next to the fact that it would be very labour insensitive, due to radioactivity of the samples it would be unacceptable from an ALARA point of view. Therefore a set of tools is designed to be able to place up to 20 samples in a tubular holder, making batch measurements possible. The tools have been designed and tested by NRG. Due to the fact that two different samples sizes were tested, two sets of tooling equipment were made. The tools are displayed in figures Figure 4-3 and Figure 4-4. The samples were counted by using a V-shaped tool. With the known average particle size, the appropriate number of particles was determined based on the length of the particle stack. The next step was filling the tubular sample holder with a funnel. During the measurements, samples had to be secured to prevent movement that disturbs the image acquisition. Plugs were design to secure the samples in the sample holder. Samples were prepared for a weeks' worth of measurement. To minimize radiation levels in the lab, the samples were stored in lead shielded sample container.

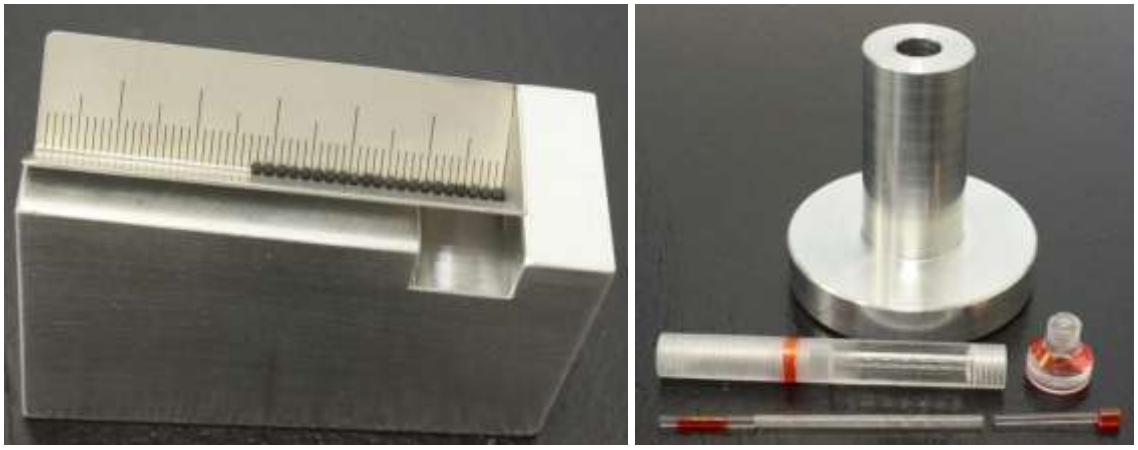

Figure 4-3: Measurement tool (left) and filling tools (right)

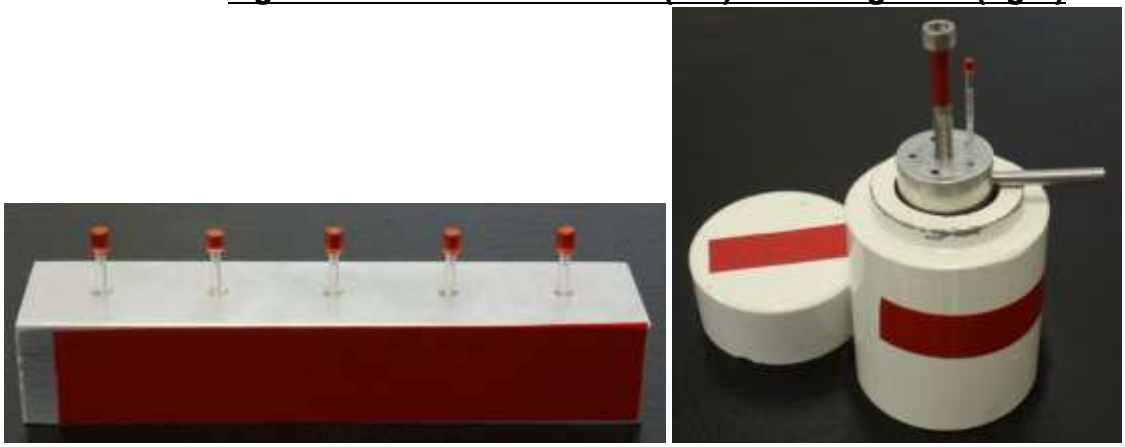

Figure 4-4: Plug holder (left) and lead shielded sample container (right)

Measurements tests have been performed on the 4 layer type particles (Kernel/buffer/SiC/PyC) as shown in Figure 3-1. The tests are performed to optimize the setup for optimal resolution and contrast. To reach this, different holder materials are tested and easy handling is investigated. The geometry of the sample holder needs to be optimized since this influences the position of the particles in the cone beam, and the holder material has its effect on the contrast that is obtained in the images. An optimized contrast is vital for distinction between the layers for the analysis of the 3D reconstruction.

4.3 Measurement

Once the sample holders are filled, the batch processing of the PYCASSO samples particles starts.
The observation ROI option is used to have the correct incident beam intensity for each individual X-Ray image that is used for reconstruction. The values used as incident beam intensity are stored in a log file during acquisition based upon a region of interest defined in the set-up phase of acquisition.

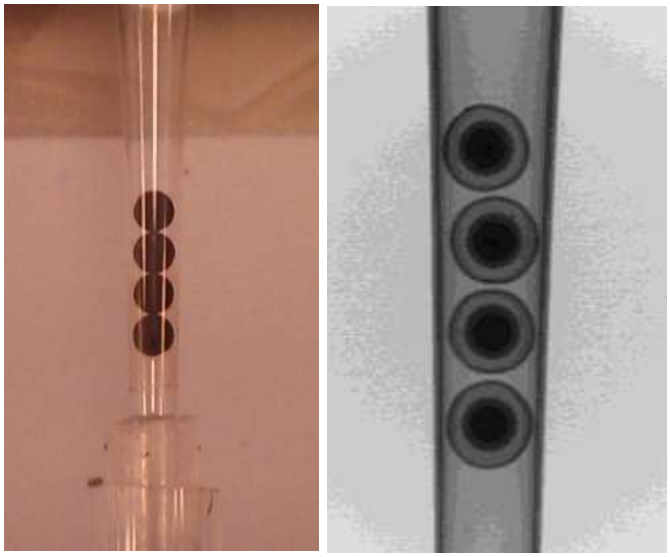

Figure 4-5: Setup and X-Ray image of unirradiated four layer type (kernel/buffer/SiC/PyC) particles (test run)

4.4 Reconstruction and data analysis

The reconstruction is based on a 360° sample rotation of 2300 frames. With the sample holder included in the reconstruction the voxel size is approximately 2. A reconstruction performed at NRG of a single particle is shown in Figure 2.

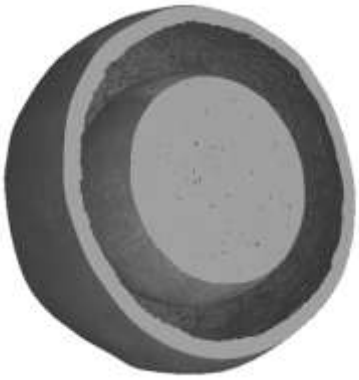

Figure 4-6: Reconstruction of the SiC layer and kernel

The reconstructions were sent to the X-Ray Imaging center of the University of Manchester where the particle analysis was performed. Each individual TRISO particle dataset was supplied as a stack of reconstructed XCT (X-ray Computed Tomography) orthoslices in a tiff file Format, as well as the reconstructed XCT voxel (3D-pixel) size. Datasets were imported into VSG Avizo 8.1 visualisation software for image filtering and particle layer segmentation. Each TRISO particle layer was then analysed using in-house MATLAB quantification code.

The visualisation software employed for data cropping, imaged filtering and segmentation was the FEI-VSG proprietary software Avizo Fire version 8.1. Details of the data segmentation are shown in section 4.4.1. The segmented volumes were then analysed using in-house MATLAB software as detailed in section 4.4.2.

4.4.1 Data preparation and segmentation

The XCT data was loaded into AVIZO as a tiff image stack using a voxel size of 1.99 microns in the x,y and z coordinates as supplied by the NRG instrument data file. Due to the combination of XCT streak artefacts and particle-to-particle contact the top and bottom 5% of each particle were removed as shown in Figure 4-7 and Figure 4-8. The latter process allows the more efficient use of automated segmentation methods and a reduction of manual corrections.

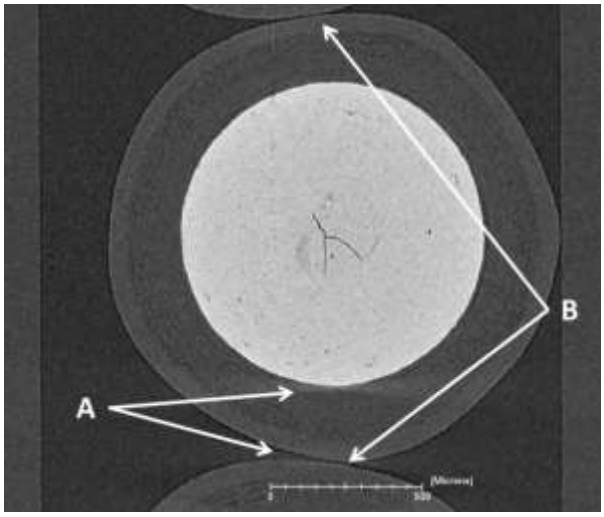

Figure 4-7 – Orthoslice (single 2D section from the 3D scan) of the raw reconstructed TRISO data. XCT streak artefacts (A) and particle contact (B) are indicated.

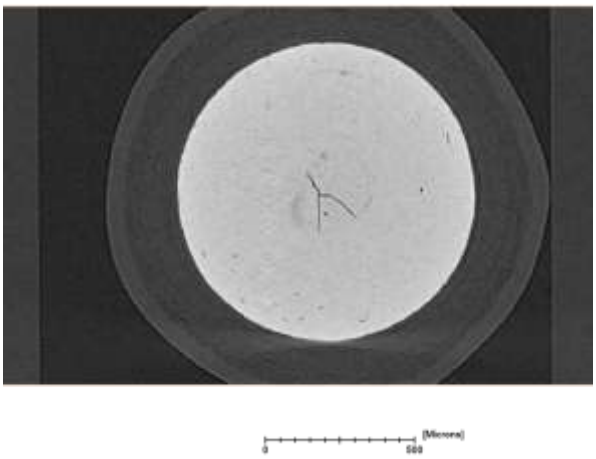

Figure 4-8– Orthoslice of the cropped reconstructed TRISO data. Note that an image filter has been applied.

The XCT data showed significant levels of noise possibly due to a limited number of projections and/or low transmission signal. Because automated segmentation methods are based upon the pixel grey scale values this noise can create significant problems. Therefore a bilateral filter was applied. The bilateral filter reduces noise in the main phases (kernel, buffer, SiC etc.) but retains material edge definition. It can be noted that a non-local means filter produces a slightly better result but requires a processing time of four hours as opposed to five minutes for the bilateral filter.

Image segmentation was carried out in a number of stages. Because the X-ray attenuation of the container and the carbon layers (OPyC and IPyC) are very similar an automated separation is not possible. The first step involved segmenting single slices of the container tube material above and below the regions where the carbon and container make contact. A segmentation interpolation was then applied to segment the tube material away from the carbon. Next the whole TRISO particle was segmented by selecting the appropriate grey scale threshold. Due to a variation of the pixel values caused by the streak artefacts at the top and/or bottom of the OPyC layer, some areas were not fully segmented. These areas were corrected manually by selecting appropriate local pixel grey scale values and then growing and shrinking the selected volume as required (Figure 4-9). Unselected regions between the kernel and the outer layer were corrected by using a combination of the voxel region growing and shrinking to close pores and the ‘remove islands’ tool in the AVIZO software.

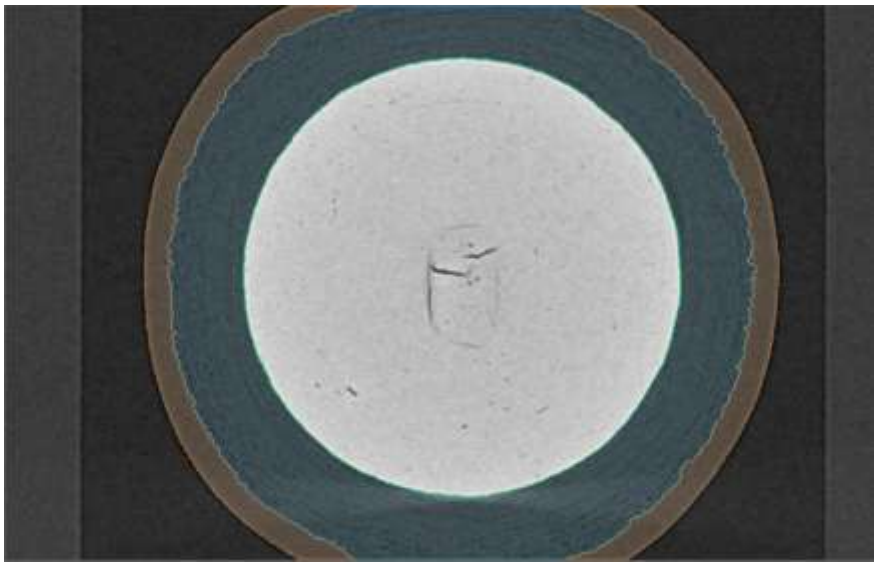

Figure 4-9 – XCT orthoslice through the centre of the TRISO particle showing the thresholding of the OPyC, SiC and buffer layers and the kernel.

For the PyC1-6_9 and PyC-M-C-6 type particles (kernel/buffer/OPyC), the buffer layer was selected by segmenting the pores within the buffer first . These regions were then grown appropriately to separate the buffer and OPyC layers. Some manual correction was required.
For PyC2-5_9-B2 type particles the SiC layer required minimal corrections near either the top or bottom of the particle depending upon the positioning of the streak artefacts. Both the buffer and kernel regions could be segmented automatically with minimal corrections. It can be noted that a number of kernels contained significant pores.
The PyC-B-C-12 and PyC-M-C-2 particles (kernel/buffer/SiC/OPyC) posed significant segmentation challenges due to the delamination. The OPyC and SiC layers of these particles were segmented as for the PyC2-5_9-B2 particles. The remaining volume was reduced into a number of shrinking spheres. These layers were then segmented upon the local thresholds to separate the buffer material from the delamination (Figure 4-9).

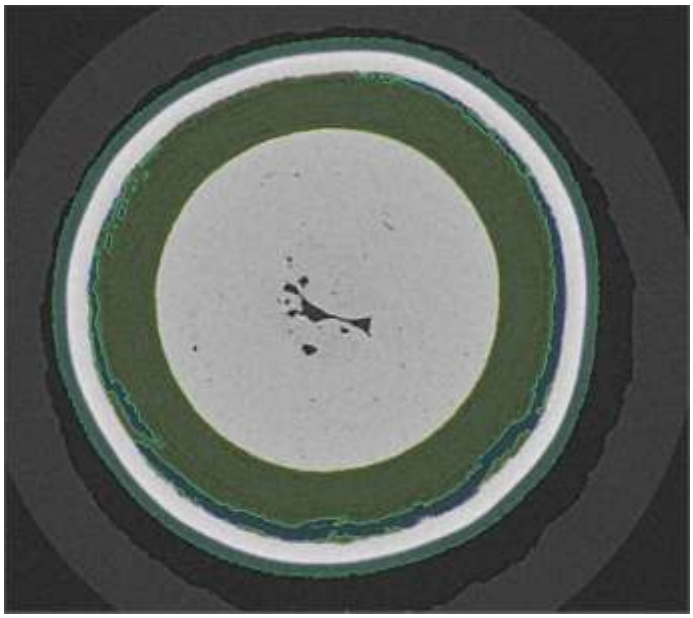

Figure 4-10 - XCT orthoslice through the centre of the TRISO particle containing a delamination. The OPyC, SiC, delamination, buffer and kernel layers have been segmented.

The segmented TRISO labels for each particle were then saved in the AVIZO visualisation software as binary data using the AVIZO file format. These files was were then read into the MATLAB analysis software described in section 5.2.

4.4.2 Data analysis

The analysis procedure, post segmentation, comprised the following steps:

1. Determine the particle centre by calculating the centre-of-mass of the kernel. Project radial lines outward from particle centre over all angles.
2. Polar angles were in the range 0 to 180°, and azimuthal angles were in the range 0 to 360°, with the angular step size being 1° for both.
3. Find the start and end of each layer along each radial line.

The following measurements were then derived for each particle (all values are in units of microns):

1. Layer thickness, as a function of polar and azimuthal angles. The data is saved in the FITS image file format (which can be opened in ImageJ) as 'file name_TDIST.fits'.
2. Distance from kernel centre-of-mass to layer mid-point, as a function of polar and azimuthal angles. This centre-to-centre distance will be referred to as 'radius'. The data is saved in the FITS file format (which can be opened in ImageJ) as 'file name_MEANDIST.fits'.
3. Mean layer thickness (average value over all angles).
4. Standard deviation of layer thickness (over all angles).
5. Mean layer radius (average value over all angles).

Measurements 3-5 are saved in excel format as 'file name_STATS.xls' for each particle. The layer thickness measure for the kernel corresponds to the kernel radius (i.e. half the kernel diameter). The standard deviation of layer thickness gives an indication of layer variability and hence roughness.

5 Results

The acquired data results in a spreadsheet form, with the measured thickness and diameter for all layers per particle, average and standard deviation. Per particle type the observations and coating behaviour will be discussed.

5.1 PYC 1

The PYC1 type particles consisted of a kernel with a buffer and PyC layer. 250 particles are measured, of which 52 were unirradiated, 97 were irradiated at the lower fluence level of $1.633 \cdot 10^{25}$ n/m^2 (E>0.18MeV), and 101 particles were irradiated at $2.025 \cdot 10^{25}$ n/m^2.

The particle size for the batch of which the unirradiated particles was determined at 1560 µm, with a standard deviation of 20 µm during fabrication. During fabrication, two methods were used to determine the particle size [2]. The first method used was by optical method [2], in which the samples were measured after each coating step, determining the obtained coating layer thickness. This is a quick and reliable method to determine the outer dimension of a large number of particles. The inner layers however are possibly altered during the coating process by abrasion. The dimensions of the inner layers are determined by destructive measurement techniques on a representative batch afterwards, by grinding to the mid-plane of the particles and determining the layer thicknesses by microscopy.

The results from the XRT measurements on the unirradiated particles are compared to the measurements before irradiation to validate the, this correlates really well with the determined outer diameter of 1560.9 µm, based on the OPyC layer diameter + the thickness. Table 5-1 to Table 5-3 show the results per batch.

Table 5-1 : PyC1-6_9_unirradiated

Fluence	0	n/m2 (E>0.18 MeV)	
	Kernel	**Buffer**	**OPyC**
Particle count [-]	52	52	52
Mean thickness [µm]	494.91	225.14	59.22
Std of thickness [µm]	1.46	9.45	2.05
Mean radius [µm]	248.45	608.43	750.86
Std of radius [µm]	0.73	4.73	9.16

Table 5-2 : PyC-B-C-6 – Low Fluence

Fluence	1.633E+25	n/m2 (E>0.18 MeV)	
	Kernel	**Buffer**	**OPyC**
Particle count [-]	97	97	97
Mean thickness [µm]	496.43	197.41	61.34
Std of thickness [µm]	2.01	8.54	2.10
Mean radius [µm]	249.33	596.19	724.41
Std of radius [µm]	0.95	4.87	9.36

Table 5-3 : PyC-M-C-6 – High Fluence

Fluence 2.025E+25 n/m2 (E>0.18 MeV)

	Kernel	Buffer	OPyC
Particle count [-]	101	101	101
Mean thickness [µm]	497.59	193.93	60.45
Std of thickness [µm]	1.70	10.38	2.41
Mean radius [µm]	249.79	595.43	722.88
Std of radius [µm]	0.85	5.53	10.61

In Figure 5-1 to Figure 5-3 the results are plotted against the reached fluence during irradiation. The error bars indicated the standard deviation per measurement point. Some clear trends are observed. The kernel seems to show consisted growth depending on the fluence, up to 0.54% radius increase at the high fluence level.

The buffer layer shows clear compaction, with a decrease of 31.2 µm in thickness, or 13.9%. Accordingly the mean radius has decreased since the kernel remained practically unchanged with an increase of only 1.3 µm, or 0.54%. The OPyC layer has shrunk accordingly to the shrinkage of the buffer layer. No debonding was observed, with the layers still well connected. The decrease in radius of the OPyC layer is therefore consistent with the decrease in buffer thickness. The thickness of the OPyC does show swelling, but with a slightly lower increase at the high fluence level. Although the trend does not appear to be linear, with the relatively large error bars no clear conclusions can be drawn.

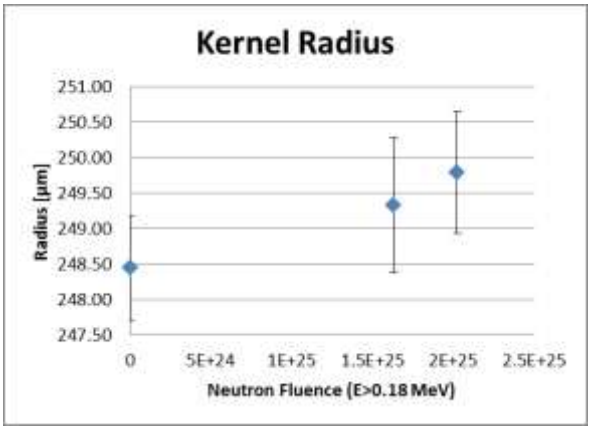

Figure 5-1: PYC1 Kernel radius

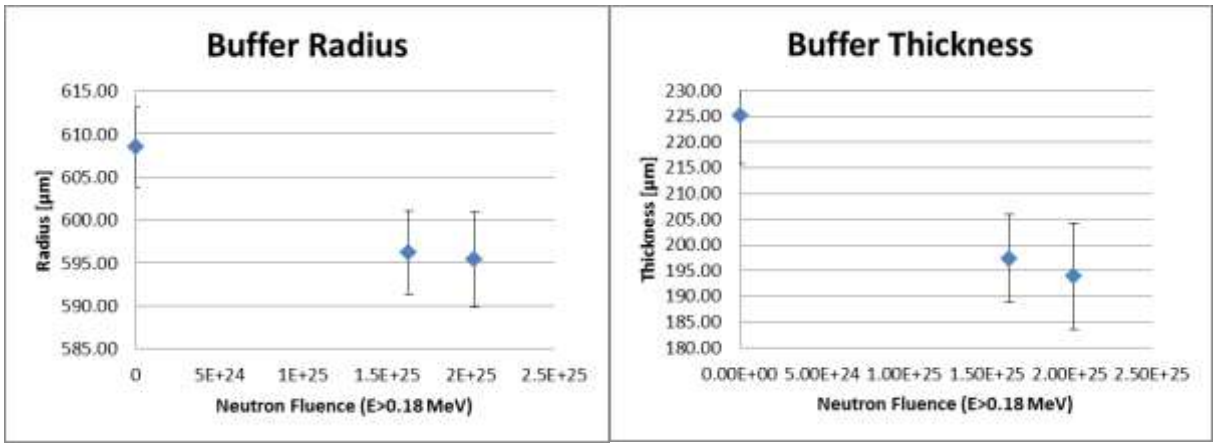

Figure 5-2: PYC1 radius and thickness of the buffer layer

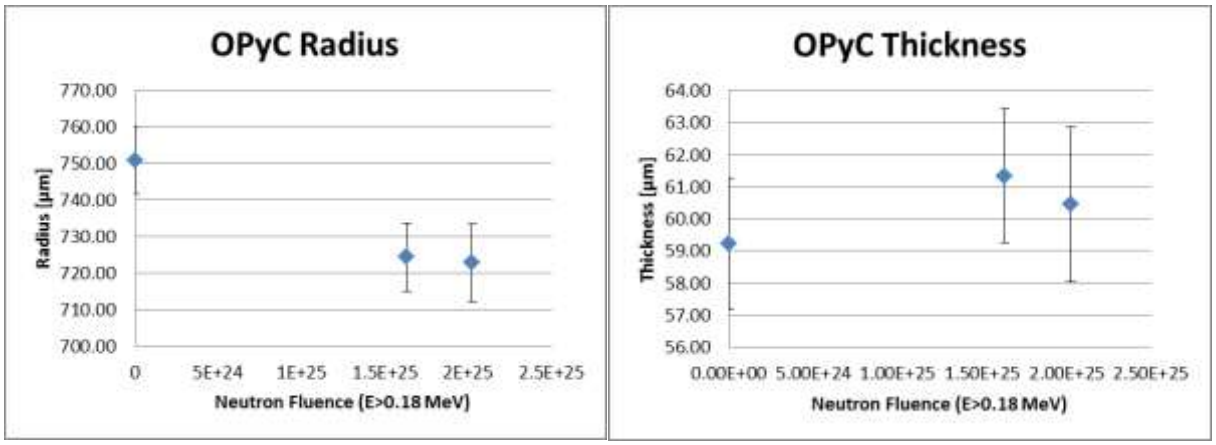

Figure 5-3: PYC1 radius and thickness of the OPyC layer

5.2 PYC 2

The PYC2 type particles consisted of a kernel with a buffer, SiC and OPyC layer. 223 particles are measured, of which 54 were unirradiated, 91 were irradiated at the lower fluence level of $1.43 \cdot 10^{25}$ n/m^2 (E>0.18MeV), and 78 particles were irradiated at the higher fluence level of $2.00 \cdot 10^{25}$ n/m^2.

The reconstructions from the irradiated PYC2 particles proved to be more complicated, due to the fact that they all showed a clear debonding layer, as shown in Figure 5-4. All particles show a clear delamination between the buffer and the SiC layer. The layers appear to be connected on one side, with the gap increasing to roughly 40-60 um on the opposite side.

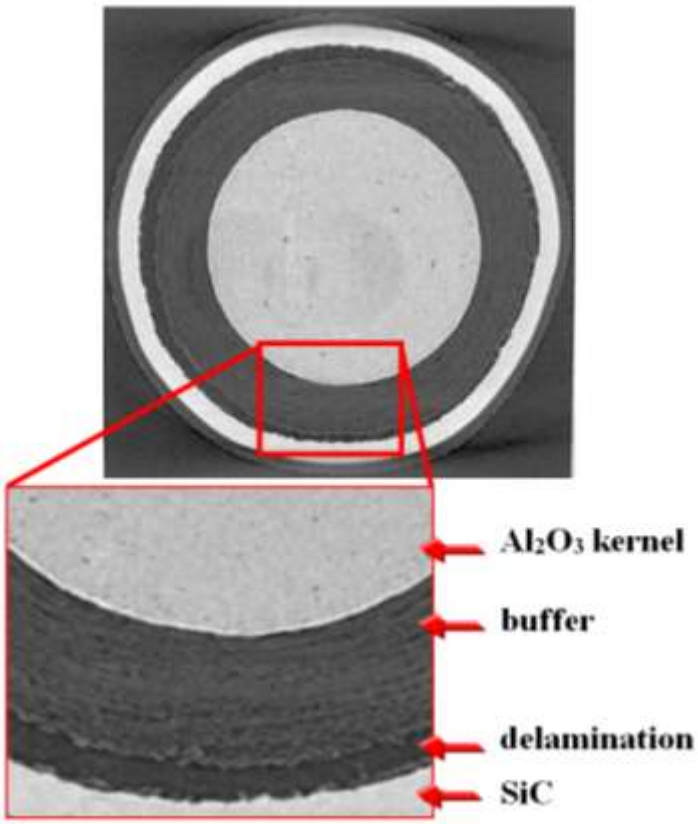

Figure 5-4: Detail of the delamination in the irradiated particle

Table 5-4 to Table 5-6 show again all the measurement data from the reconstructed XCT data. During fabrication the total particle size was determined at 1573 µm with a standard deviation of 20 µm. From the reconstruction a value of 1574.2 was determined based on the OPyC layer diameter + the thickness showing again a good correlating between the two measurement methods.

Table 5-4 : PyC2 - Unirradiated

Fluence 0

	Kernel	Buffer	Delamination	SiC	OPyC
Particle count [-]	54	54	n/a	54	54
Mean thickness [µm]	492.37	190.55	-	63.37	38.44
Std of thickness [µm]	1.71	10.80	-	1.30	2.10
Mean radius [µm]	247.18	588.57	-	716.87	767.88
Std of radius [µm]	0.86	5.34	-	10.18	9.77

Table 5-5 PyC-B-C-12 – Low Fluence

Fluence 1.43E+25 n/m2 (E>0.18 MeV)

	Kernel	Buffer	Delamination	SiC	OPyC
Particle count [-]	91	91	91	91	91
Mean thickness [µm]	494.06	155.24	26.11	64.60	35.85
Std of thickness [µm]	1.81	9.20	2.01	1.28	2.14
Mean radius [µm]	248.03	572.66	663.26	715.36	765.68
Std of radius [µm]	0.90	5.06	9.78	9.83	9.50

Table 5-6 PyC-M-C-2 – High Fluence

Fluence 2.00E+25 n/m2 (E>0.18 MeV)

	Kernel	Buffer	Delamination	SiC	OPyC
Particle count [-]	78	78	78	78	78
Mean thickness [µm]	494.79	154.56	28.69	63.72	36.34
Std of thickness [µm]	1.64	8.66	2.36	1.55	2.07
Mean radius [µm]	248.39	573.04	664.68	717.97	768.00
Std of radius [µm]	0.82	4.40	9.11	9.86	9.55

Figure 5-5 to Figure 5-9 show the measured radii and thicknesses plotted against the received neutron fluence. The error bars indicate the standard deviation per measurement point. Again some clear trends can be observed.

A similar amount of swelling is observed for the kernel to that of the PYC1 particles. At high fluence the relative increase is 0.49%, similar to the PYC1 relative change. The same decrease in buffer thickness is observed in the PYC2 series, with a decrease in thickness up to 36 µm, or 18.9%. In these particles however the next layer is SiC, which has maintained its original size. The change in radius is negligible, and although at the lower fluence level some thickness increase is observed, at the high fluence level it is almost zero.

The OPyC layer also shows no change in radius, being held in place by the SiC beneath it. The thickness however has decreased noticeably, by 6.8 and 5.5% at the lower and high fluence level, respectively.

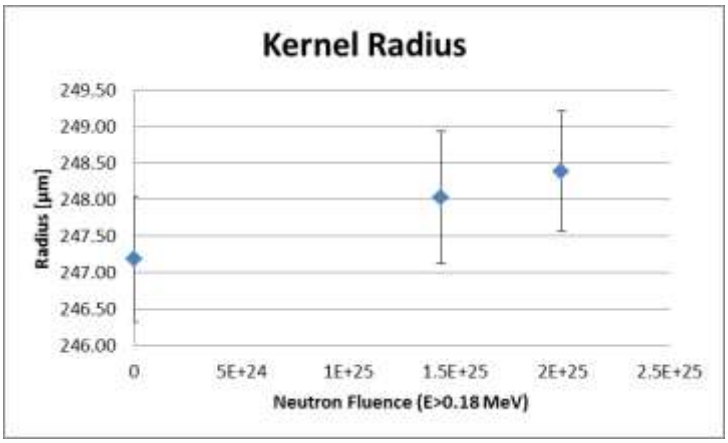

Figure 5-5: PYC2 kernel radius

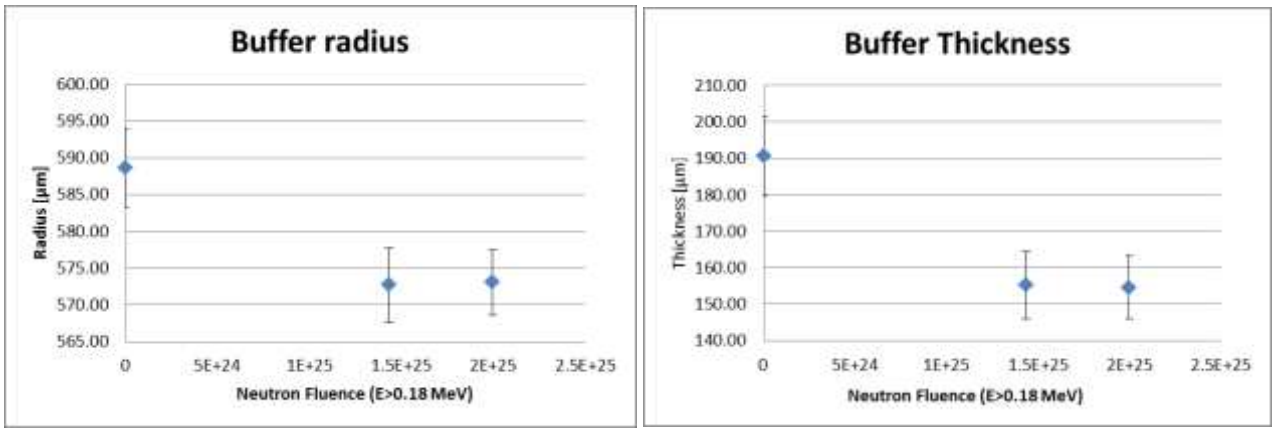

Figure 5-6: PYC2 radius and thickness of the buffer layer

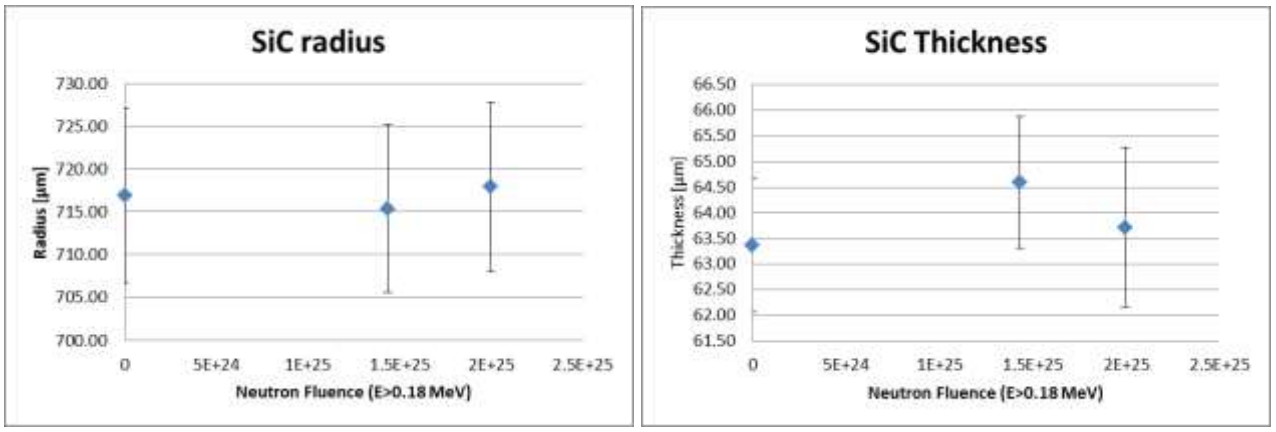

Figure 5-7: PYC2 radius and thickness of the SiC layer

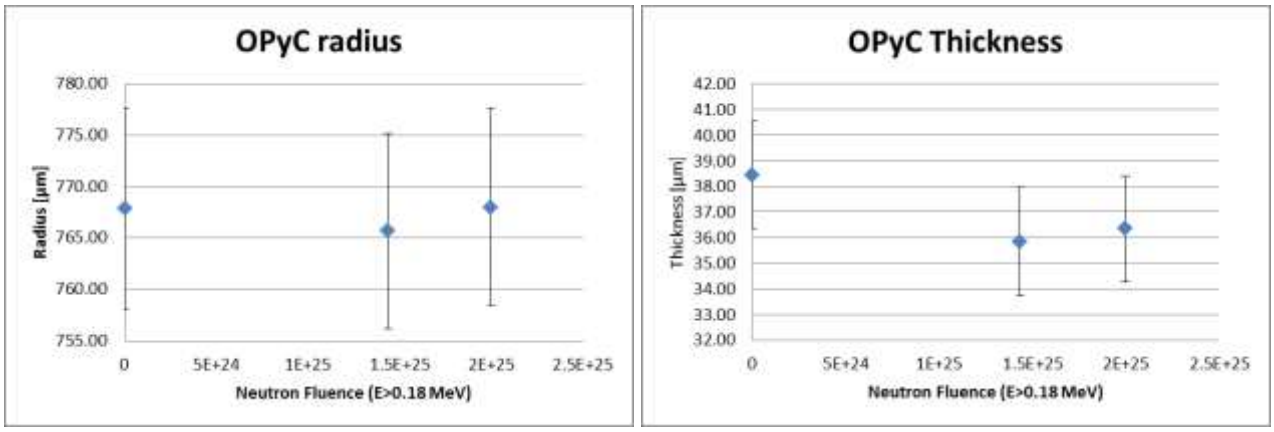

Figure 5-8: PYC2 radius and thickness of the OPyC layer

Finally also the delamination layer is plotted. Obviously, the standard deviation within each delaminated layer is quite significant (not listed in the table) due to the fact that the thickness of the layer is zero on one side, and has a maximum on the opposite side. The average size however is consistent with a relatively small standard deviation.

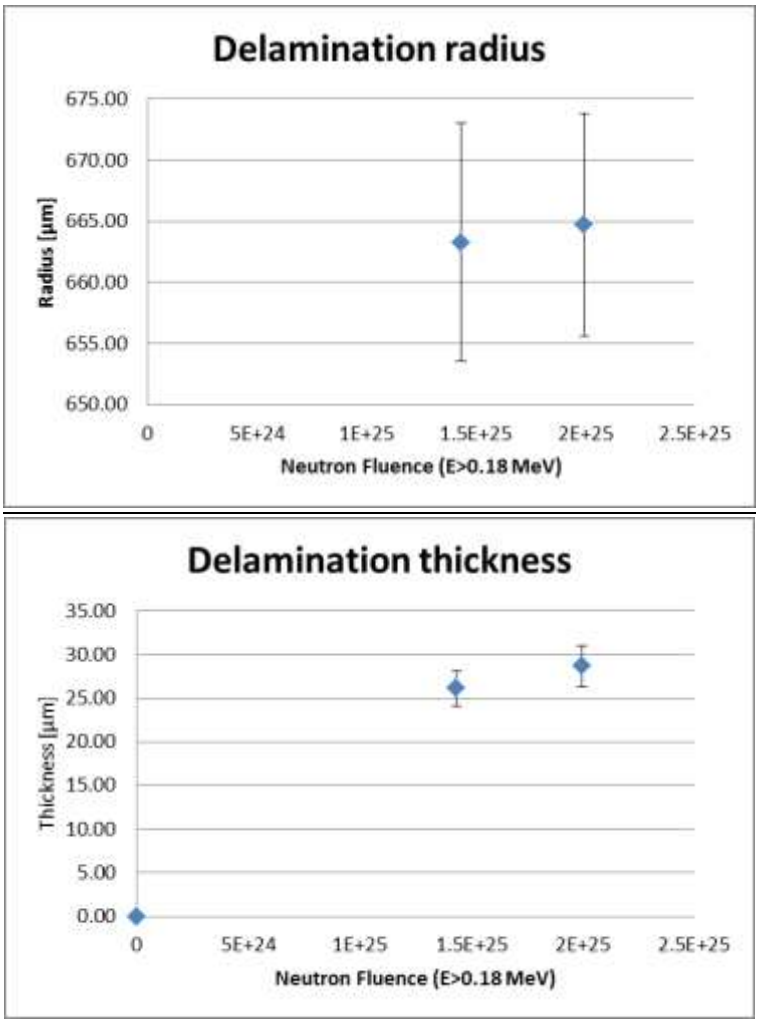

Figure 5-9: PYC2 radius and thickness delamination layer

6 Conclusions

Close to 500 particles have been measured by X-Ray Tomography at NRG. The results show consistent results with the coating sizes measured during fabrication, showing a consistent result between the two methods.
The technique allows to study a large number of particles to be studied non-destructively, for which a batch process was developed and used. With this new process, it was made possible to scan particles continuously during day and night.

The XRT measurements were performed at NRG and data was analysed by the University of Manchester. The results show a clear difference between the two types of particles that were studies. The particles that consisted of a kernel, buffer layer and OPyC layer clearly showed shrinkage in the two graphite layers. The buffer is known to shrink, but without any restraint, the OPyC layer follows the buffer layer, shrinking up to 3.7% in radius, whilst increasing up to 3.5% in thickness.
The second type of particle with a SiC layer between the two graphite layers, clearly restrains the OPyC layer. The buffer shows similar behaviour, shinking significantly in size, the SiC remains unchanged, also keeping the OPyC layer in place. In this case, the OPyC layer does shrink significantly in thickness, up to 6.75%.

7 Acknowledgement

The authors would like to thank the ARCHER project and the ministry of Economic Affairs from the Netherlands for funding this work.

The data image cutting, filtering and segmentation were performed by Mr Xuekun Lu, Miss Bo Yu, Mr Xun Zhang and Miss Ying Wang. This work was supervised and directed by Dr Tristan Lowe whereas the data analysis using MATLAB was performed by Dr Robert Bradley.

Reference List

[1] FP6 "RAPHAEL" ReActor for Process heat, Hydrogen And ELectricity generation, in: Contract Number: 516508 (FI6O) ed., 2005.

[2] FP7 "ARCHER" Advanced High Temperature Reactors for Cogeneration of Heat and Electricity R&D, in: Contract no. 269892 ed., 2011.

[3] M.Perez, F.Charollais, PYCASSO Sample and Test Speciment Fabrication Report, in: RAPHAEL-0408-D-FT2-4 ed., 2008.

[4] S.Knol, S.de Groot, P.R.Hania, M.H.C.Hannink, PYCASSO: Irradiation of HTR coated particles at high temperatures, Nuclear Engineering and Design In Press, Available Online (2011).